Global and flexible models for Sodium-cooled Fast Reactors in fuel cycle simulations

M. Ernoult, X. Doligez, Nicolas Thiollière, A.A. Zakari-Issoufou, A. Bidaud, S. Bouneau, J.B. Clavel, F. Courtin, S. David, A. Somaini

GLOBAL AND FLEXIBLE MODELS FOR SODIUM-COOLED FAST REACTORS IN FUEL CYCLE SIMULATIONS

M. Ernoult[1], X. Doligez[1], N. Thiollière[2], A.A. Zakari-Issoufou[1] A. Bidaud[3], S. Bouneau[1], J.B. Clavel[4], F. Courtin[2], S. David[1], A. Somaini[1]

[1]Institut de Physique Nucleaire, IN2P3/CNRS-Université Paris Sud
Orsay, France
[2]Subatech, IMTA-IN2P3/CNRS-Université de Nantes
Nantes, France
[3]LPSC, IN2P3/CNRS-UGA-Grenoble INP
Grenoble, France
[4]LN, IRSN/PSN-EXP/SNC
Fontenay-aux-Roses, France

ernoult@ipno.in2p3.fr
Institut de Physique Nucleaire,
15 rue Georges CLEMENCEAU
91406 ORSAY (FRANCE)

Abstract

Since Sodium cooled Fast Reactors are present in many scenarios and strategies for the future of nuclear energy while not having a specific design established yet, we created a new fast and flexible model for the dynamic fuel cycle simulation tools CLASS. It includes a depletion meta-model and a fuel loading method based on artificial neural networks. It is able to represent a wide range of Sodium cooled Fast Reactor designs using oxide fuels and a wide range of fuel management strategies within fuel cycle simulation tools. A comprehensive analysis of simplification options has been made in order to choose the right level of complexity for the reference full core depletion calculations performed with the MURE code used for the training of the meta-model. The process from these reference calculations to the final meta-model is explained and a specific focus is given to the operations going from

Preprint submitted to Annals of Nuclear Energy:VSI:PHYSOR-2018 December 21, 2018

detailed full core depletion results to global results suitable for neural networks training. Details on the creation process for neural networks based predictors, one for each average cross-section, and their training on full core depletion calculations are given as well as the implementation within the CLASS code. The irradiation meta-model achieves good precision on all major and minor actinides present in spent fuel. The designs and loaded fuel covered by the model allow significant burner to strong breeder strategies. A sensitivity analysis shows that the number of fertile blankets is the primary contributor for breeding capabilities, but effects of isotopic composition are also significant. A test scenario illustrates the model capacity to simulate burner and breeder designs.

Keywords: sodium-cooled fast reactor, fuel cycle, breeding ratio, meta-model
PACS: 28.41.Vx, 28.50.Ft, 89.30.Gg

---

1. INTRODUCTION

Sodium cooled Fast Reactors (SFR) are present in many scenarios and strategies for the future of nuclear energy. They regularly represent a large part of future nuclear reactor fleets, sometimes up to 100%. Thus, it is essential to include models for these reactors in fuel cycle simulation codes. However, the deployment of SFRs at the industrial scale has not started yet. A wide range of designs are still studied [1, 2, 3, 4, 5, 6, 7]. Their technology readiness level are very wide and go from ideas to almost industrial reactors. To conclude about scenarios including these reactor concepts, we need models within fuel cycle simulation codes, models precise enough to render the sensitivity of isotopes' inventories to changes of designs and/or recycling strategies. Creating one model for each design and then testing all scenarios with all models would be unnecessarily time-consuming considering how far most sodium fast reactor concepts are from industrial technology readiness levels.

To avoid this problem while still providing a model precise enough to conclude on scenarios involving SFRs, we choose to develop a single, physics-based, flexible model able to represent a wide range of SFR designs and core physics. In this flexible model many design parameters (such as the radius or the height of the active core or the fertile blankets) are not set but can be chosen during scenario design. This enables to adapt the SFR design

in each scenario and to reach break-even, burner or breeder performances while using the same model and thus enabling continuous exploratory and prospective studies. However, some other designs parameters have been fixed because the difficulty of continuous change between options: the fuel of the reactor always remains purely oxides; the fuel lattice pattern always remains hexagonal and fuel assembly are built using the same fresh fuel composition throughout all their height.

2. CREATE A TRAINING BASE FOR META-MODELS

The meta-models described in this paper are primarily constructed to be used in the dynamic fuel cycle simulation code CLASS [8].

To create these meta-models, we used a method inspired by methods used to create CLASS's previous meta-models [9, 10] based on neural networks trained over numerous depletion calculations. First, in subsection 2.1, we present the considered base designs and the changes we made on it. Then in subsection 2.2, we present several modeling simplifications made in our reference calculation. And at last in subsection 2.3 some other assumptions are clarified.

2.1. Range Of Design

To represent a range of SFR designs as wide as possible while maintaining the continuity and unity of our meta-model, we choose one base SFR concept and then introduced a range of variations on several key design parameters to add flexibility. The base concept used is the sodium cooled large size fast neutron reactor core described in a NEA Benchmark [11]. It's a core designed by CEA [6] using oxide fuel ($(U, Pu)O_2$) and close to the SFR V2B concept with a nominal thermal power of $3600 MW_{th}$.

To explore a wide range of reactor sizes, we varied radius and height of the active core around the benchmark's values (see table 8 in section 3.2 for exact range boundaries). This opened breeder and burner configurations in addition to the break-even initial concept. To avoid the need of studies on mechanical behavior of the fuel of in thermo-hydraulics of the cooling system, power density and assembly geometry have not been changed. These variations of reactor size lead to thermal powers from $900 MW$ to $6500 MW$.

An inner core and an outer core with different Pu fractions are considered. The Pu fractions in these two regions vary independently within a limit : the ratio between the two fractions should never be far from 1.

The volume ratio between different core zones with different Pu ratios is not constant between the different existing SFR's designs. In all considered designs, it was fixed: $\frac{V_{out}}{V_{in}} = 1.04$. The radius of the inner active core is adjusted proportionally to the total radius to maintain this volume ratio.

Furthermore, studied designs can have from 0 to 3 full rings of fertile blanket assemblies around the active core. Blanket assemblies are similar to active cores assemblies but use depleted uranium instead of fuel.

Two examples of designs illustrating the possible range are shown in Figure 1 : one large and one small core, one with blankets and one without.

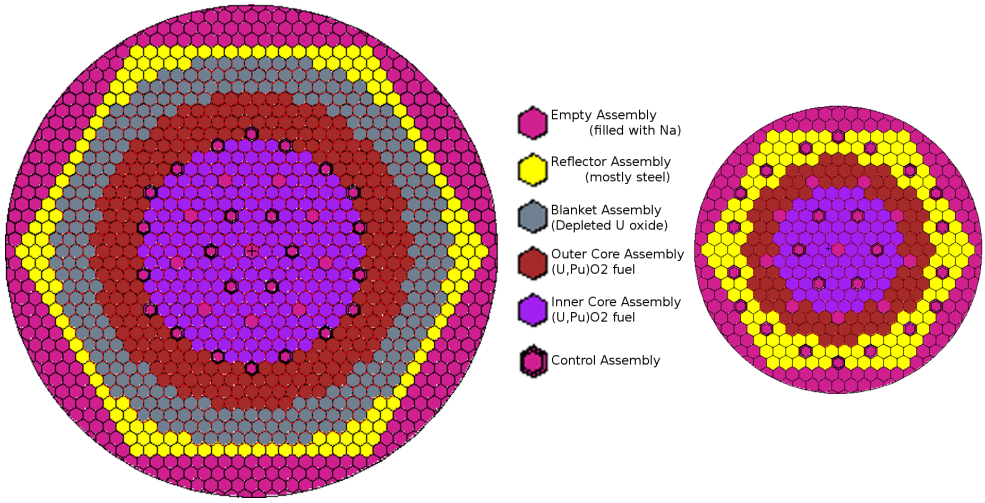

Figure 1: Two Examples of Core designs used for the training base : The large core on the left has 3 blanket rings and a radius of $2m$ and the small core on the right has no blankets and a radius of $1.5m$.

2.2. Simplification For The Reference Simulations

To train our neural network based predictors, reference calculations spread throughout the considered designs need to be performed. These calculations have all been performed with MURE [12], a code using various Monte-Carlo solvers to solve transport equations and a Runge-Kutta 4 method for Bateman equation resolution developed at CNRS.

The construction of our meta-model needs a big number of reference calculations to be well-trained over all the range of the considered designs, therefore numerous full core depletion calculations are needed to create a

database on which meta-models could be trained. To optimize the calculation cost of the creation of this training base, several modeling simplifications have been evaluated regarding their effect on precision and calculation cost.

2.2.1. Statistical effects

The MURE code is based on Monte-Carlo transport solver (MCNP [13] or Serpent [14]) therefore all of its results are riddled with statistical errors. Because the meta-model is to be used in fuel cycle simulation, one of the requirement is to predict with precision the criticality level of the core in order to adjust correctly the amount of fissile in fresh fuels. To assure that, we adjusted the number of active neutrons of the MC code to have less than $100pcm$ of statistical uncertainties on the multiplication factor. 75 full core calculation were then made to evaluate the uncertainties on the depletion. The reactivity swing between the beginning and the end of irradiation has shown to have an associated statistical error of $150pcm$. Representing around 3% of the typical reactivity swing.

This choice of statistics leads to the errors of less than 0.1% on actinides' inventories at the end of irradiation for all actinides, even for heavier minor actinides.

2.2.2. Full core calculation

When creating meta-models, simulation of the full core is often avoided and only one assembly of the reactor surrounded by reflective boundaries is then simulated [8, 15, 10]. In thermal reactors, these calculations represent relatively well the behavior of a full core [16]. However, since neutron's mean free path in fast reactors is far bigger, larger than characteristic dimension of assemblies, such simplification thus leads to significant deviation on the inventories. To quantify this bias, two calculations have been made using geometrical and materials data from the reference design: with only one assembly and with a full core.

A significant effect is observed. The multiplication factor of the assembly calculation is $2000pcm$ higher than the one of the full core. The actinides' inventories at the end of irradiation were vastly different, with difference higher than 50% for several major Pu isotopes. Due to these large biases, we chose to always use full core calculation, during the creation of the training base and the simplifications tests.

The full core calculation from this subsection, using none of the following analyzed simplifications, simulate exactly the benchmark design [11]. It is

the reference calculation for all following studies.

2.2.3. Homogenized assemblies

If the high mean free path of neutrons in fast reactors forbid the use of assembly calculation as a base for our meta-models, it leads to a lesser sensitivity of neutronic behavior to small dimension geometry details. To take advantage of this property, we evaluated the use of homogenized assemblies in the core, that is using only one cell per assembly containing a mixture of cladding, sodium and fuel. This simplification allows a huge reduction in the number of cells to consider in simulation and thus the computation cost is divided by 4.

^{238}U	^{244}Cm	^{242}Cm	^{243}Am	^{241}Am
0.07%	-0.61%	-0.03%	-0.39%	0.02%
^{242}Pu	^{241}Pu	^{240}Pu	^{239}Pu	^{238}Pu
0.04%	-0.06%	-0.07%	-0.35%	0.07%

Table 1: **Bias on actinides' inventories at the end of irradiation when using homogenized assemblies compared to the reference full core calculation**

The comparison of a full core simulation with detailed geometry and one with homogenized assemblies showed a small deviation on actinides' inventories at the end of irradiation as detailed on table 1 : only 0.5% for each actinide except for ^{244}Cm (0.6%). The effect on the multiplication factor is around $250pcm$, less than 3 times the statistical uncertainty ($100pcm$) and therefore indistinguishable from statistical variations.

Such biases have been considered low enough and all following simulations have been made with homogenized assemblies.

2.2.4. Multigroups cross-sections

In order to decrease this calculation cost, an option to use multi-group cross-sections (using on 17 900 groups) has been developed in MURE as in [17]. This allows to get one multi-group flux from the MC code instead of each individual cross section independently, and makes the calculation approximately 20% faster. This option can be used for all cross sections or an exception can be made for cross-sections of ^{238}U.

The effect of both options on actinides' inventories at the end of irradiation is presented in table 2. In both cases, the errors introduced are lower than 1% on all actinides. However, the use of multi-group for ^{238}U leads to

	^{238}U	^{244}Cm	^{242}Cm	^{243}Am	^{241}Am
for all	0.08%	0.76%	0.56%	0.58%	-0.45%
except for ^{238}U	-0.01%	0.09%	0.47%	0.25%	-0.16%
	^{242}Pu	^{241}Pu	^{240}Pu	^{239}Pu	^{238}Pu
for all	-0.06%	-0.17%	-0.05%	-0.58%	-0.12%
except for ^{238}U	-0.01%	-0.10%	0.04%	0.03%	-0.01%

Table 2: **Bias on actinides' inventories at the end of irradiation when using multigroup cross-sections compared to the reference full core calculation**

an error of 0.6% on ^{239}Pu that is decreased to 0.03% when making an exception for ^{238}U. This significant precision gain doesn't impact significantly the calculation cost.

For the multiplication factor, observed difference is less than $30pcm$, lower than the statistical error, for both options.

Because of time gain and the low bias, the multi-group option with an exception for ^{238}U has been used for all simulations.

2.2.5. Time discretization

The number of time steps, that is the frequency at which cross-section are updated using MC transport calculation during the depletion, increase the calculation cost. Simulations with 128 time steps have been considered as a reference, since adding more time steps into the simulation has no observable effect.

Time steps	^{238}U	^{244}Cm	^{242}Cm	^{243}Am	^{241}Am
2	0.04%	3.77%	1.95%	1.48%	0.37%
12	0.01%	0.30%	0.16%	0.27%	0.11%
Time steps	^{242}Pu	^{241}Pu	^{240}Pu	^{239}Pu	^{238}Pu
2	0.10%	1.24%	0.76%	0.60%	0.12%
12	0.02%	0.001%	0.01%	0.06%	0.05%

Table 3: **Bias on actinides' inventories at the end of irradiation when 2 or 12 time steps compared to 128**

Table 3 shows the bias introduced on inventories when reducing the number of time steps simulated. A too low number of time steps, 2 for example, causes significant bias : more than 1% for some Pu isotopes. But 12 time steps allow a good precision : a bias lower than 0.1% on EOC inventories

of U and Pu and 0.2% on EOC inventories of minor actinides. For the multiplication factor, the use of 2 time steps already result in a difference indistinguishable from statistical variations ($248pcm$). Using 12 time steps lowers this difference to $90pcm$. Because of this low bias and a reasonable calculation cost, 12 time steps have been used in all following simulations.

2.2.6. Spatial discretization

Plutonium repartition. : In the chosen reactor designs at the start of the irradiation, there are two different zones with two different Pu ratios. To check if these 2 zones with different ratios should be simulated separately, several calculations have been made in a core divided in 9 radial zones with different repartition while keeping the same total amount of Pu in the core.

^{238}U	^{244}Cm	^{242}Cm	^{243}Am	^{241}Am
-0.13%	-3.87%	-0.31%	2.92%	-2.02%
^{242}Pu	^{241}Pu	^{240}Pu	^{239}Pu	^{238}Pu
0.00%	-1.04%	0.31%	1.00%	-0.83%

Table 4: **Bias on actinides' inventories at the end of irradiation when using only average Pu content compared to taking into account the 2 Pu content zones of the concept, both option using 9 radial depletion zones**

Table 4 shows the difference between two of the tested options : a completely flat Pu repartition in the core or the repartition of the concept design (2 zones with the outer one having 20% more Pu than the inner one). The errors are higher than 1% on some Pu isotopes but remain relatively low. However, k_{eff} evolution is completely different, the reactivity swing with flat distribution is 35% lower than the one of the design concept. Therefore, the heterogeneous distribution of the Pu at the beginning of the irradiation has to be kept in the calculation used to train our meta-model.

Number of radial zones. : To keep the initial Pu distribution at least 2 radial zones are needed. To check if more depletion zone are needed, a comparison has been made between a 2 zones calculation and another one where each of these 2 zones were divided in 3 sub-zones (total of 6 depletion zones).

Table 5 shows errors on major actinides below 1% and on minor actinides below 3%. Using this simplification, the k_{eff} at the end of irradiation shows a difference of $596pcm$. This value stays within 3 standard deviation of statistical uncertainties (statistical error of a difference between two values

^{238}U	^{244}Cm	^{242}Cm	^{243}Am	^{241}Am
-0.06%	-1.61%	1.67%	2.46%	-2.00%
^{242}Pu	^{241}Pu	^{240}Pu	^{239}Pu	^{238}Pu
-0.02%	-0.73%	0.20%	0.45%	-0.82%

Table 5: **Difference on actinides' inventories at the end of irradiation with 2 zones or 6 zones (2 groups of 3 zones each)**

with each having a statistical uncertainty of $100pcm$ is $200pcm$). The bias caused by this simplification has been considered acceptable within the goal of our meta-model when compared to the decrease of calculation cost allowed. Therefor only 2 depletion zones were used in the active core for the training of our meta-model. When fertile blankets were used, a third depletion zone was added.

2.3. Modeling Choices For The Reference Simulations

Outside of these simplifications adopted because of their small enough influence, two major hypotheses have been made during the calculation for the training base.

2.3.1. Refueling patterns

For SFRs, no fuel loading pattern seems to make consensus. For this reason we choose the simplest refueling pattern possible : a one batch core.

To evaluate the bias introduced by such modeling choice, we studied the difference between a core using the batching in fifth and a core without batching. For the batched core, each of the two fuel zones is separately batched by fifth. In each zone, the 5 batches of assemblies have been arranged in a checked pattern so that average burn-up of a random group of neighboring assemblies stay as close to the core average as possible.

The main goal of batching is to reduce the reactivity swing. A core refueled in 5 batches has a reactivity swing approximately 5 times smaller than a core without batches. However, a polynomial fit of the k_{eff} from a non-batched depletion can be recombined and give a good estimate of the k_{eff} of a batched depletion [18]. Such reconstruction leads to a bias on the reactivity swing of around 15%.

Furthermore, the cross talk between assemblies leads to differences in the neutron spectrum within the assemblies and thus differences on actinides' inventories at the end of irradiation. These differences are presented in table 6.

^{238}U	^{244}Cm	^{242}Cm	^{243}Am	^{241}Am
-0.16%	3.50%	0.08%	1.55%	-1.30%
^{242}Pu	^{241}Pu	^{240}Pu	^{239}Pu	^{238}Pu
-0.28%	-0.14%	0.16%	-0.07%	-0.85%

Table 6: **Difference between 1 batch and 5 batches refueling patterns on actinides' inventories at the end of irradiation**

Thanks to the fast spectrum, cross-sections have only small variations during irradiation, and these differences are small : less than 1% on U and Pu and 4% for minors actinides. For inventories the non-modeling of batching has thus a limited effect.

2.3.2. Reactivity control

In almost all fast reactor designs, the reactivity is controlled only through control rods. Choosing the right position for control rods require complex models and prediction schemes that are not fully available in our code. For this reason, the simulation has been made with control rods completely removed from the core. The reactivity of the simulated core is not controlled and it is overcritical during part of the irradiation.

To evaluate the bias introduced, we studied the difference between all the control rods fully inserted during the whole irradiation and all the control rods fully removed of the core.

^{238}U	^{244}Cm	^{242}Cm	^{243}Am	^{241}Am
0.20%	-6.01%	-1.10%	-3.03%	0.52%
^{242}Pu	^{241}Pu	^{240}Pu	^{239}Pu	^{238}Pu
-0.34%	-1.52%	-1.61%	-0.60%	0.17%

Table 7: **Difference between absence and presence of reactivity control on inventories of actinides at the end of irradiation**

The capture of neutron by the control rods is not uniform, neither spatially nor energetically. Thus, neutron spectrum changes and the relative flux of the different zones of the reactor are impacted by the presence or absence of control rods. The difference between these two cases on major isotopes at the end of irradiation is shown in table 7 to be higher than 1.5% on several Pu isotopes and up to 6% for Cm. These biases are not negligible, specifically in studies where these elements could be recycled, but we don't have

the technical capabilities to perform a real reactivity control. Furthermore, gap between our simulation without control rods and a realistic option are most probably lower that these values because during operation control rods are moving in and out of the core and don't stay fully inserted.

3. META-MODELS CREATION

Using options presented in the previous section, depletion calculations have been made with MURE [12]. Once the calculations representative of all considered possible configurations performed, the effective creation of the meta-models starts. The subsection 3.1 describes the transformation of MURE results into files usable by neural network trainers. After, in subsection 3.2 the training of the meta-model is explained. The implementation of the models in the scenario code CLASS [8] are then described in section 3.3.

3.1. Agglomeration Of The Results

Until now the models used in CLASS were based on depletion calculation with one evolving cell [9, 10].

The analysis of simplifications presented in the previous section led us here to keep three different depletion zones.

However, to decrease calculation time, our depletion meta-model calculates global inventories using global averaged cross sections and a Bateman equation solver. Our predictors need thus to be trained at each time step on only one value per physics observable (flux, cross-sections, isotopic compositions and k_{eff}), a value that should enable to recalculate the evolution of the global isotopic quantities in the full core, N^i_{glob} which are the total inventory of isotope i in the core. The three cells of our full core depletion calculation (inner active core, outer active core and fertile blankets) have widely different Pu fractions and flux level. Therefore, a special care should be taken when calculating the global values.

Inventories are extensive variables, so for each isotope, at each time step the global value is the sum of all values : $N^i_{glob} = \sum_c N^i_c$, where N^i_c is the inventory of this isotope in the fuel cell c.

The flux corresponds to the total length traveled by all neutrons per unit time and volume in an intensive variable therefore the global flux for the full core is an average weighted by the volume. At each time step $\phi_{glob} = \frac{1}{V_{glob}} \sum_c \phi_c V_c$, where ϕ_{glob} is the global flux in the core, ϕ_c the flux in the fuel

cell c, V_{glob} is the total volume of the core and V_c the volume of the fuel cell c.

The last global variables are the cross sections. To calculate average global cross-sections, we calculate the global reaction rate for each reaction on each isotope. Reaction rates are extensive variables so the global value is the sum of all values : $RR^{i,r}_{glob} = \sum_c RR^{i,r}_c$, where $RR^{i,r}_{glob}$ is the total reaction rate of isotope i for reaction r in the core and $RR^{i,r}_c$ is the reaction rate of this isotope in the fuel cell c. Then using the fact that $RR = N\sigma\phi$, we can calculate global cross sections σ_{glob} : for each reaction for each isotope, at each time step $\sigma^{i,r}_{glob} = \frac{RR^{i,r}_{glob}}{N^{i,r}_{glob}\phi_{glob}}$.

For the fuel creation method, the only physical parameter considered is the multiplication factor k_{eff} that is a global parameter and thus doesn't need any condensation.

All this agglomeration of physics variables have been automated so the result of the depletion calculations can be automatically transformed into files combining all the data needed for the mean cross section predictor training and testing.

3.2. MLP Training

To create the mean cross sections predictor from the training base, like in previous CLASS models [9, 10], neural networks of the multi-layer perceptron type have been used. For that purpose, we used the TMVA library [19] developed within the ROOT package [20]. The depletion meta-model is based on one independent neural network for each cross section with 13 input parameters presented in table 8. Only the average Pu isotopic composition of the total fresh fuel is given. The isotopic composition of the inner and outer fuel is calculated using the Pu_{Out}/Pu_{glob} ratio. The same Pu isotopic composition is used for both of the fuel. Only the total proportion of Pu is adjusted.

Latin hypercube sampling [21] has been used to create 1500 sets of input parameters paving the whole input parameter's phase space and a depletion calculation made for each of them. From the 1500 calculations, 750 were randomly chosen for training these neural networks and the 750 others were used for testing.

Training time is negligible compared to the time needed to create the training base so a conservatively large number of neurons on two hidden layers has been used (40 neurons of the first hidden layer and 20 on the

Parameter	Unit	min	max	Comment
Radius	m	1.5	3	for the active core
Height	m	0.7	1.3	for the active core
Blankets	rings	0	3	Fertile blankets
Pu_{Out}/Pu_{glob}	Ratio % Pu	0.9	1.5	outer-core over average
235U	% mol in HM	0.1	0.2	in the total fresh fuel
238U	% mol in HM	74	96	in total fresh fuel
238Pu	% mol in HM	0	2.4	in total fresh fuel
239Pu	% mol in HM	1.3	19	in total fresh fuel
240Pu	% mol in HM	0.5	13	in total fresh fuel
241Pu	% mol in HM	0	5	in total fresh fuel
242Pu	% mol in HM	0	5	in total fresh fuel
241Am	% mol in HM	0	2.5	in total fresh fuel
Time	days	0.0	2050	Irradiation time

Table 8: **Neural network input parameters and ranges used**

second) and the BFGS method was used for weights adjustment. To decrease the risk of over-training, the regulator provided in the TMVA ROOT package have been used.

A similar neural network has been trained to predict the multiplication factor, k_{eff}, in the beginning of the irradiation.

3.3. Meta-model Implementation

Using these predictors, the meta-models have been implemented within the CLASS code. The depletion meta-model performs an irradiation simulation. At each time step, Bateman's matrices are created using cross section predicted by our mean cross sections predictors. Then inventories for the next time step are calculated by solving Bateman's equation with Runge-Kutta fourth-order method.

The fuel creation method uses the multiplication factor predictor. Like in [10], the average Pu content needed to achieve a given k_{eff} at the beginning of the irradiation is determined by a dichotomy and multiple calls of the predictor. In burner reactors, k_{eff} tends to decrease. To achieve the most efficient burning, we want a high k_{eff} while still being able to control the reactivity. In SFR the main reactivity control mechanisms are control rods. The total reactivity of all the control rods in our designs are between $4000pcm$ and $6000pcm$ (higher for smaller cores because we keep the same number of

control assemblies) as for most large SFR designs [22]. For safety purpose only half of the control rods length should be used in normal control situation, which leads to maximum acceptable reactivity swing of $3000pcm$, not far from values used in SFR core design [7]. Therefore, in burner reactors, we aim at $k_{eff}(t = 0) = 1.03$ without reactivity control. In breeder reactors, k_{eff} tends to increase, so we aim at $k_{eff}(t = 0) = 1$. The meta-model then ensures that $k_{eff} \leq 1.03$ and thus keeping the reactor in a controllable state.

4. MODEL EVALUATION

4.1. Model's Precision

To estimate the error on isotopic inventories, we compared the inventories at the end of irradiation of the 1500 MURE calculations with the ones calculated with our meta-model for the same fresh fuel composition. Only half of these calculations has been used for the training of the neural networks predictors so an over-training would lead to the appearance of two distinct groups of errors in the results : with small errors for the training data and with higher errors for the test data. Each MURE calculation takes around 30 h while each meta-model calculation takes less than 1 minute (both on 1 CPU). Figure 2 shows that for U and Pu the differences between the two codes on EOC inventories are 4% at maximum. For other significant nuclei (that is isotopes with a proportion greater than 1ppm in the irradiated assemblies' composition that includes cladding and coolant, that is around 1 pcm in the spent fuel and some hundred of grams) the differences are 15% at maximum. All the errors are grouped and no distinction between the training data and the test data is visible, so we are confident that our predictors are not over-trained.

The multiplication factor predictor has also been tested. The error calculated by making the difference between the k_{eff} given by MCNP during the first step of the MURE depletion calculation and the prediction by our meta-model. This errors average value is $-80pcm$ and its standard deviation is $553pcm$. The average error is lower that the statistical uncertainty on the k_{eff} in the MURE calculation ($100pcm$) and therefore indistinguishable from statistical variations. The standard deviation of the error is a little larger that what could be expected from statistical variations, however higher errors are concentrated for extreme values of k_{eff} that should be avoided thanks to our meta-model targeting k_{eff} between 1.0 and 1.03. We therefore consider

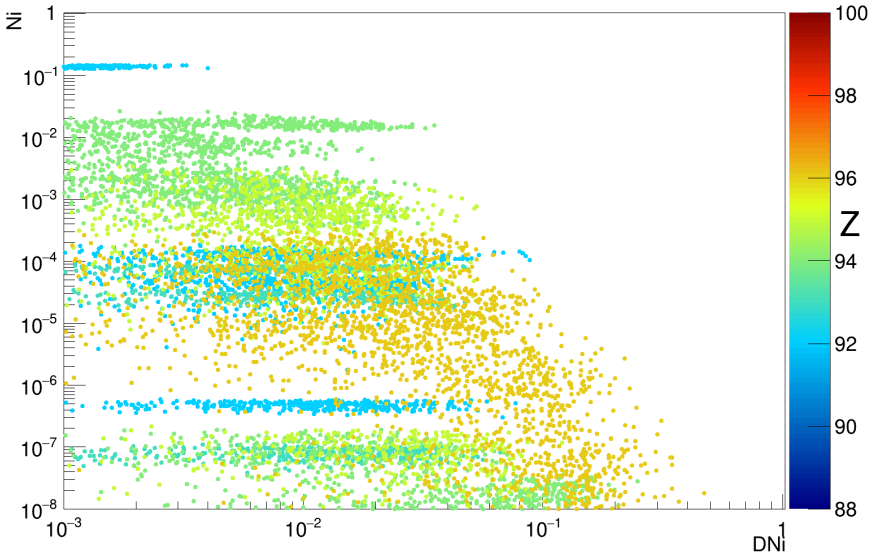

Figure 2: Comparison of MURE and CLASS prediction for EOC actinides inventories for 1500 different fresh fuel compositions. DN_i is the relative difference between CLASS and MURE calculation. N_i is the proportion of nuclei in the spent fuel. Color of the dots represent the Z of the isotope it represents

the precision of the multiplication factor predictor enough for our need in fuel cycle simulations.

4.2. Analysis of Breeding ratio range and sensitivities

In this work the breeding ratio (BR) has been calculated by the formula $BR = \frac{Pu(t=tf)}{Pu(t=0)}$. All isotopes of Pu have been considered equivalent for this purpose and no decay of ^{241}Pu during the unavoidable cooling phase is taken into account. No decay of ^{239}Np is considered in this BR evaluation.

To evaluate feasible BRs in the considered SFR designs, we limited ourselves to the same situations that we considered feasible for the average Pu fraction in section 3.3.

With these limitations, we get BRs from 0.88 to 1.41 with higher frequency of the ones around 1.0. This BR distribution seems to be well fitted with common uses of SFR in scenarios : allowing significant burning or breeding while giving most detailed description and flexibility for SFR near break-even.

To better understand the role of the designs parameters and the fresh

fuel composition on the BR, we calculated sensitivities of the BR to all these parameters using standardized regression coefficients methods [23] within R code [24] : $S = \frac{\delta k/k}{\delta X/X}$. They have been calculated for the subset of reference calculations, which are critical in the beginning of the irradiation and have a reactivity swing lower than $3000pcm$ for similar reasons as explained in 3.3. Table 9 shows that the number of blankets rings is of primary importance for determining the BR but other parameters have also a big influence. During irradiation the proportion of each isotope tends to get closer to its equilibrium value. Therefore, the decrease of BR with the increase of initial Pu fraction is expected. Because of the selection considering k_{eff}, an increase of even Pu isotopes is correlated with an increase of the Pu fraction to compensate the criticality. Therefore, the negative sensitivity for all even Pu isotopes is explained the same way. The positive sensitivities of the odd Pu isotopes have the same origin.

	R	**H**	**Blankets**	**% Pu**	$Pu_{Out}/Pu_{average}$	
Sens.	0.08	0.36	4.28	-0.32	0.38	
	% ^{238}Pu	% ^{239}Pu	% ^{240}Pu	% ^{241}Pu	% ^{242}Pu	% ^{241}Am
Sens.	-0.02	0.38	-0.33	0.10	-0.15	0.02

Table 9: **Sensitivity of BR to various entry parameters**

The non negligible influence of Pu isotopic composition on BR leads to the possibility for BRs' variations with a fixed design. A reactor with a $BR = 1.05$ with a Pu rich in ^{239}Pu will see it go below 1 using a Pu with a significantly lower amount of ^{239}Pu (or ^{241}Pu).

4.3. Breeding ratio prediction

In scenarios studies, BR of a fast reactor is often more significant than precise design. To help choose design parameters, we designed a formula giving an estimate of the BR from the fixed design parameters, (the radius and the height of the active core as well as the number of blankets rings). Because it also depends significantly on the isotopic composition of the Pu used as a fissile material, any formula using only the fixed design parameters could not predict exactly which BR will be achieved in the scenario. Knowing this impossibility of a predictive formula, we choose a second order polynomial function, which allows extracting informations and intuitions from the values of its coefficients instead of an artificial neural network that could get better

precision but with neurons weight that are not understandable. A chi square minimization gave the value of the coefficients for the final formula:

$$\begin{aligned} BR = \quad & -0.854 + 0.292R + 3.048H + 0.002B \\ & -0.014R^2 - 1.278H^2 - 0.005B^2 \\ & -0.209RH - 0.008RB + 0.059HB \end{aligned} \tag{4.1}$$

where **R**,**H** and **B** represent the **R**adius, **H**eight and number of **B**lankets.

This formula predicts a $BR = 0.96$ for a burner SFR with $R = 3m$, $H = 0.7m$ and no blankets, and a $BR = 1.09$ for a breeder SFR with $R = 1.5m$, $H = 1.3m$ and 3 rings of blankets.

These BRs are estimated without any consideration for the Pu isotopic vector, they should not be seen as predictive quantitative value but only as generic burner/breeder tendency. To test their validity and calculate the true BRs of these two designs we will now simulate these designs in a full scale scenario.

5. SCENARIO APPLICATIONS

5.1. Definition of an Example Scenario

To test our model, we adapted the scenario used as a base for uncertainties analysis in the NEA benchmark of 2016 [25].

Our scenario considered a transition from a fleet of PWR UOX to a fleet of SFR that multi-recycle the Pu produced during UOX irradiation. The total duration of our scenario is 300 years. The fleet starts with only PWR UOX. From year 100, UOX PWRs start to be replaced regularly by SFRs so that, in year 130, all the PWRs have been replaced. Compared to the scenario of the benchmark, we increased the duration of the initial phase from 80 to 100 years to be sure to have enough Pu to start our SFRs, and we added 100 years at the end to have a clear picture of the full SFR fleet behavior. The fuel cycle characteristics are taken from the NEA benchmark. However, the reactor designs of the PWR UOX and SFR used were not the one specified in the benchmark but the one available in CLASS. The UOX PWR used standard French 900MWth PWR models for depletion and fuel creation. A target burn-up of $60GWd/tHM$ was used for these UOX PWRs. The SFR used the meta-models presented here.

In order to test the range of our meta-models, two scenarios have been simulated. One using each of the SFR designs presented at the end of the last section 4.3 : a *Burner Scenario* using a SFR with $R = 3m$, $H = 0.7m$ and

no blankets (predicted $BR = 0.96$) and a *Breeder Scenario* using $R = 1.5m$, $H = 1.3m$ and 3 rings of blankets (predicted $BR = 1.09$). To decrease the calculation time in these sample scenarios, we choose not to model each reactor separately but only two macro-reactors, one PWR and one SFR whose powers are changed through the scenario. The effect of the size of reactors on the depletion calculation is still taken into account into the cross-sections.

5.2. Results and Breeding Ratio Calculations

The two scenarios have been simulated with CLASS [8] using our new models.

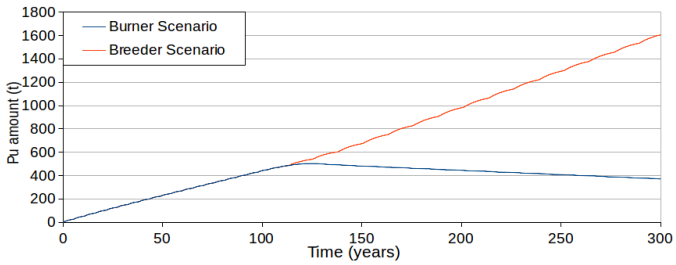

Figure 3: Evolution of the total amount of plutonium in the burner and breeder scenarios

Figure 3 shows the evolution of the total amount of plutonium in the whole fuel cycle, including plutonium in the reactors, cooling pools and storage facilities. Both scenarios are identical during the first phase, Pu quantities increase during irradiation of UOX fuels. During the second phase when the SFRs start, the scenarios diverge. In the burner scenario, Pu is decreasing during all this phase while it is increasing in the breeder scenario. Total Pu inventory at the end of the breeder scenario is almost 4 times higher than at the end of the burner scenario. Figure 4 shows the achieved power in both scenarios. In both scenarios, there are small power spikes appearing between 100 and 130 years due to impossibilities to decrease the power of reactor in the middle of irradiation. In the burner scenario, we see jumps between full power and zero power : the power of the fleet is not guaranteed. This comes from fuel loading failure due to insufficient Pu in the stock. This effect is amplified by our use of one macro-SFR so either the full fleet starts or no reactor starts at all.

Using the evolution of the global Pu inventories, we can calculate average effective BRs. We set the average effective breeding ratio $< BR >$ as :

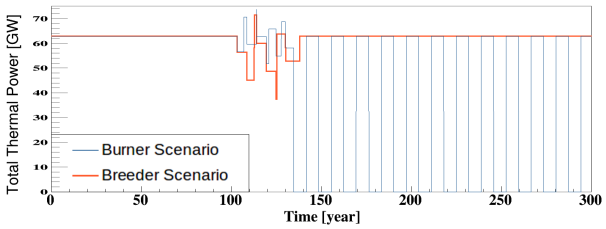

Figure 4: Evolution of the total power in the burner and breeder scenarios

$(< BR >)^N = Pu(T_f)/Pu(T_0)$ where T_0 is the start of the considered period, T_f the end of the considered period and N is the number of cores loaded in the reactor during this period. Failed loading in the burner scenario are taken into account by decreasing the number of cores loaded.

For the *Burner Scenario*, the fast reactor has $< BR >= 0.99$ between 150 and 200 years, and $< BR >= 0.98$ between 200 and 300 years. For the *Breeder Scenario*, $< BR >= 1.09$ between 150 and 200 years, and $< BR >= 1.04$ between 200 and 300 years. This change of BR during the scenario without any change of the design is due to the effect on Pu isotopic vector in the BR. This effect is rendered in our model thanks to the resolution of Bateman equations during the fuel cycle simulation with global cross sections adapted to the isotopic content of fresh fuel.

The SFR in the burner scenario is effectively a burner SFR and the one in the breeder scenario is a breeder : the generic tendency is well predicted by the formula (4.1), and we showed that our model can simulate both burner and breeder SFRs. The BRs are not far from the ones predicted, but because of the fit method, it's impossible to guarantee such good prediction in all cases and therefore formula (4.1) should only be used to predict the burner/breeder tendency and not to give numerical value of BRs.

6. CONCLUSIONS

In this work we presented a new flexible model, including a depletion meta-model and a fuel loading meta-model, able to represent a wide range of Sodium cooled Fast Reactors designs and its implementation within the fuel cycle simulation tool CLASS. We explained the process of creation of neural networks based predictors, one for each average one group cross-section and one multiplication factor, and their training on 750 full core depletion

calculation made with the MURE code. During these depletion calculations several simplification hypothesis have been used to decrease calculation time however it has been checked that the biases stay below 1% on the end of cycle actinides composition. These checks of simplification options have notably shown that full core simulation are needed at each step but that homogenization is possible within assemblies. Throughout calculating global values using equations that guarantee the conservation of global isotopic evolution. We translated localized results from the depletion calculation to global results usable for neural networks training and presented the implementation of the models within the CLASS code. Precision of the global irradiation meta-model has been tested. The model achieves precision better than 4% on all major actinides in spent fuel. The breeding ratios of designs covered by the model go from 0.88 (burner) to 1.41 (breeder) with the most design diversity close to break-even. A sensitivity analysis showed that the number of fertile blankets is the primary contributor for determining breeding capabilities. The effects of isotopic composition of fresh fuel are also significant, leading the prediction of a breeding ratio change. A synthetic formula that evaluates the breeding ratio as a function of SFR radius, height and number of blankets is given. A full mathematical treatment of two sample designs (corresponding to a breeder and a burner) shows that the simplified model presented here is indeed satisfactory.

REFERENCES

[1] G. Flamenbaum *et al.*, "Superphnix core-loading strategy using the checkerboard pattern," *Nuclear Science and Engineering*, vol. 106, pp. 11–17, 1990.

[2] V. Poplavsky *et al.*, "Core design and fuel cycle of advanced fast reactor with sodium coolant," in *International conference on fast reactors and related fuel cycles*, (Kyoto, JAPAN), 2009.

[3] T. Ellis *et al.*, "Traveling-wave reactors : a truly sustainable and full-scale resource for global energy needs," in *ICAPP*, (San Diego CA, USA), 2010.

[4] L. Buiron *et al.*, "Innovative core design for generation iv sodium-cooled fast reactors," in *ICAPP*, (Nice, FRANCE), 2007.

[5] P. LeCoz *et al.*, "Sodium-cooled fast reactors: the astrid plant project," in *ICAPP*, (Nice, FRANCE), 2011.

[6] P. Sciora *et al.*, "A break even oxide fuel core for an innovative french sodium-cooled fast reactor: Neutronic studies results," in *Global*, (Paris, France), 2009.

[7] K. Ammar, *Multi-physics and multi-objective design of heterogeneous SFR core : development of an optimization method under uncertainty.* Paris-Sud University, France: PhD Thesis in French, 2014.

[8] B. Mouginot *et al.*, "Core library for advanced scenario simulation, c.l.a.s.s. : Principle and application," in *PHYSOR*, (Kyoto, Japan), 2014.

[9] B. Leniau *et al.*, "Generation of sfr physics models for the nuclear fuel cycle code class," in *PHYSOR*, (Sun Valley ID, USA), 2016.

[10] F. Courtin *et al.*, "Neutronic predictors for pwr fuelled with multi-recycled plutonium and applications with the fuel cycle simulation too class," *Progress in Nuclear Energy*, vol. 100, pp. 33–47, 2017.

[11] Working Party on Scientific Issues of Reactor Systems, *Benchmark for Neutronic Analysis of Sodium-cooled Fast Reactor Cores with Various Fuel Types and Core Sizes Expert Group on Reactor Physics and Advanced Nuclear Systems.* OECD NEA/NSC/R(2015)9, 2016.

[12] O. Meplan *et al.*, "Mure : Mcnp utility for reactor evolution - description of the methods, first applications and results," in *ENC*, (Paris, France), 2005.

[13] X.-. M. C. Team, *MCNP - A General N-Particle Transport Code, Version 5.* LA-UR-03-1987, 2003.

[14] J. Leppanen *et al.*, "The Serpent Monte Carlo code: Status, development and applications in 2013," *Annals of Nuclear Energy*, vol. 82, pp. 142–150, 2014.

[15] B. Leniau *et al.*, "Neural network approach for burn-up calculation and its application to the dynamic fuel cycle code class," *Annals of Nuclear Energy*, vol. 81, pp. 125–133, 2015.

[16] A. Somaini, *Analysis of error imped by simplified modelisation on the depletion of PWR fuels*. Paris-Sud University, France: PhD Thesis in French, 2017.

[17] W. Haeck and B. Verboomen, "An optimum approach to monte carlo burn-up," *Nuclear science and engineering*, vol. 156, pp. 180–196, 2007.

[18] R. Sogbadji, *Neutronic study of the mono-recycling of americium in PWR and of the core conversion in MNSR using the MURE code*. Paris-Sud University, France: PhD Thesis, 2012.

[19] A. Hoecker *et al.*, *TMVA - Toolkit for Multivariate Data Analysis*. CERN, 2009.

[20] R. Brun and F. Rademakers, "Root: An object oriented data analysis framework," *Nuclear Instruments and Methods in Physics Research*, vol. 389, pp. 81–86, 1997.

[21] K. Ye, "Orthogonal column Latin hypercubes and their application in computer experiments," *Journal of the American Statistical Association*, vol. 93, pp. 1430–1439, 1998.

[22] R. Rachamin *et al.*, "Neutronic analysis of sfr core with helios-2, serpent, and dyn3d codes," *Annals of Nuclear Energy*, vol. 55, pp. 194–204, 2013.

[23] O. Asserin *et al.*, "Global sensitivity analysis in welding simulations -what are the material data you really need?," *Finite Elements in Analysis and Design*, vol. 47, pp. 1004–1016, 2001.

[24] R Development Core Team, *R: A Language and Environment for Statistical Computing*. R Foundation for Statistical Computing, Vienna, Austria, 2008.

[25] Working Party on the Scientific Issues of the Fuel Cycle, *The Effects of the Uncertainty of Input Parameters on Nuclear Fuel Cycle Scenario Studies*. OECD NEA/NSC/R(2016)4, 2017.